International Journal of Pharmaceutics 404 (2011) 110–115

Contents lists available at ScienceDirect

International Journal of Pharmaceutics

journal homepage: www.elsevier.com/locate/ijpharm

Electrohydrodynamic preparation of polymeric drug-carrier particles: Mapping of the process

Marjan Enayati, Uthumankandu Farook, Mohan Edirisinghe*, Eleanor Stride

Department of Mechanical Engineering, University College London, Torrington Place, London WC1E 7JE, UK

ARTICLE INFO

Article history:
Received 8 October 2010
Received in revised form 5 November 2010
Accepted 9 November 2010
Available online 17 November 2010

Keywords:
Drug carrier
Microbubbling
Biocompatible
Polymer
Size
Polydispersivity
Size distribution
Submicrometre

ABSTRACT

Submicrometre size spheres prepared from biocompatible polymers are becoming increasingly popular in drug and gene delivery. This paper describes the preparation of polymeric spheres with a mean diameter of 0.4 μm with a polydispersivity index of 8%, using coaxial electrohydrodynamic atomization (CEHDA) microbubbling. An 18 wt.% solution of polymethylsilsesquioxane, a hydrophobic biocompatible polymer, was subjected to CEHDA microbubbling by passing air through the inner needle and polymer solution through the outer needle of a twin needle co-axial device, under the influence of an electric field. A parametric plot of the flow rate of air and the flow rate of polymer solution was constructed and used for systematic process control to reduce the diameter of the microspheres from micrometre size to submicrometre size. CEHDA is an excellent method for obtaining polymer microspheres. By studying the process in detail and mapping it, we can now demonstrate it can also be used to prepare submicrometre sized particles with the ability to control size and polydispersivity.

1. Introduction

Polymer-based carriers such as bubbles, capsules and other particles are finding increasing use in a diverse range of clinical applications, e.g. for diagnostic imaging, tissue engineering and drug delivery (Lee and Lee, 2010; Chang et al., 2010a; Enayati et al., 2010; Hettiarachchi and Lee, 2010). Some of the major advantages of polymer-based drug delivery systems; are the continuous maintenance of drug levels in a therapeutically desirable range, reduction of harmful side effects, decreased amount of drug needed, and decreased size and frequency of doses (Mitragotri and Lahann, 2009). An ideal drug delivery system should be non-toxic, biocompatible, mechanically strong, capable of achieving a high drug loading, safe from accidental release, simple to administer and easy to fabricate and sterilize (Brannon-Peppas, 1997).

The influence of particle size on carrier function has been widely investigated. Particle diameter can be controlled via the physical properties of the materials or via the processing parameters of the fabrication method. Size has a great impact on many aspects of particle function such as flow properties, clearance, degradation and cellular uptake mechanisms (Stolnik et al., 1995; Dunne et al., 2000; Patil et al., 2001; Lamprecht et al., 2001). For example, micrometre-size carriers have been administered via intravascular, inhalation, nasal and subcutaneous routes and undissolved micrometre-size carriers are eventually cleared from the body mainly by phagocytosis, which is one of the body's innate modes of defence against invading pathogens and other non-indigenous particulate matter (Tabata and Ikada, 1990; Rejman et al., 2004; May and Machesky, 2001). Also, the diameter of particles administered dictates their velocity, diffusion and adhesion to walls, in blood vessels, airways or the gastro-intestinal tract (Moghimi and Hunter, 2001; Illum et al., 1982; Desai et al., 1996; Desai et al., 1997). Movement of particles in tissues, whether arriving by migration, or injection, is also limited by size due to steric hindrance in the extracellular matrix. The sub-micrometre size carrier offers a number of distinct advantages over larger microparticles, for example higher intracellular uptake (Zauner et al., 2001; Sahoo et al., 2002), being able to penetrate throughout the submucosal layers (the larger micrometre-size carriers are predominantly localized in the epithelial lining) and administration into systemic circulation without the problems of particle aggregation or blockage of fine blood capillaries.

Polymeric carriers are versatile and a range of polymeric materials such as polysiloxanes, polyethylene glycol, polylactides and polyanhydrides are employed for drug delivery because of their desirable physical properties. The choice of polymer determines several aspects of the carrier including the types of drug or protein that can be encapsulated, the mode of degradation and drug release, biocompatibility and physical properties (Uhrich et al., 1999; Pillai and Panchagnula, 2001; Panyam et al., 2003; Khutoryanskiy, 2007;

* Corresponding author.
E-mail address: m.edirisinghe@ucl.ac.uk (M. Edirisinghe).

0378-5173/$ – see front matter © 2010 Elsevier B.V. All rights reserved.
doi:10.1016/j.ijpharm.2010.11.014

Blanco et al., 2000). For instance, polymethylsilsesquioxane polymer is hydrophobic, chemically stable and unreactive and has been used *in vivo* on account of its biodurability and biocompatibility for several decades. Also, biodegradable polymers such as polylactide (PLA) homopolymers and copolymers have been extensively investigated as they have been shown to stimulate no adverse tissue reactions when carrying drugs and can be hydrolyzed in the body to form products that can be easily eliminated so that the removal of these implants by surgery is not needed (Arbós et al., 2002; Jalil and Nixon, 1990; Wang et al., 1999).

A variety of methods including emulsion-evaporation, emulsion-diffusion, breaking-up of a liquid stream, interfacial polymerization and emulsion polymerization are used for the preparation of the polymeric carriers (Bibby et al., 1999a,b; Langer, 1990; Jain, 2000; Park et al., 1998). Amongst the methods based on breaking up of a liquid jet, electrohydrodynamic atomization (EHDA) and co-axial electrohydrodynamic atomization (CEHDA), have been successfully adapted to prepare polymeric carriers including bubbles and capsules that can be used as drug delivery systems (Farook et al., 2007a; Farook et al., 2008; He, 2008). These methods offer great potential for producing multi-layered coated bubbles for use in targeted drug delivery (Jaworek, 2007). For instance, paclitaxel capsules of controllable morphology were prepared using EHDA (Xie et al., 2006). Recently, a method combining flow-focusing and laminar jet break-up has been reported to have prepared matrix structured near-monodisperse microcapsules (Stride and Edirisinghe, 2008).

CEHDA also offers ample potential for the preparation of composite microspheres, for example preparing polydimethylsiloxane (PDMS)-coated starch/bovine serum albumin (BSA) microspheres of 5–6 μm diameter (Pareta and Edirisinghe, 2006). This method can be successfully used to prepare near monodisperse spherical microcapsules by encapsulating bovine serum albumin (BSA) using poly-L-lactide (PLA) (Xu and Hanna, 2008). Using CEHDA microbubbling and using a polymethylsilsesquioxane solution, an *in situ* preparation method for liquid-filled polymeric microspheres with a mean diameter of 1.5 μm and a standard deviation of 0.5 μm has been developed (Farook et al., 2008).

The objective of this paper was to investigate the potential of the CEHDA method for controlling crucial parameters such as carrier diameter and polydispersivity. A parametric plot was constructed between the applied flow rate of air and the flow rate of polymer solution. It was used for the selection of flow rates to reduce the diameter of the microspheres from micrometre size to submicrometre size. In this paper we conform to the FDA accepted definition of nano (i.e. <100 nm) and therefore the carriers prepared are described as microspheres.

2. Materials and methods

2.1. Materials

Commercially available polymethylsilsesquioxane (density 1240 kg m^{-3}, PMS MK powder, Wacker Chemie AG, Germany) was used. General purpose research grade ethanol (790 kg m^{-3}, BDH Laboratory Supplies, UK) was used as the solvent medium and a solution of 18 wt.% polymer was prepared in a conical flask by dissolving polymethylsilsesquioxane in ethanol and by subsequently magnetic stirring for 600 s.

2.2. Characterization of solution

Density was measured using a standard 50 ml specific gravity bottle and the surface tension value was obtained using a Kruss Tensiometer (Standard Wilhelmy's plate method). Electrical conductivity was estimated using a HI-8733 (Hanna Instruments, Atlanta, USA) conductivity probe and the viscosity was determined using a U-tube viscometer (BS/U type). These characterizations were conducted at ambient temperature (22 °C) after calibrating the equipment using ethanol. Full details of these characterization methods have been published previously (Farook et al., 2008).

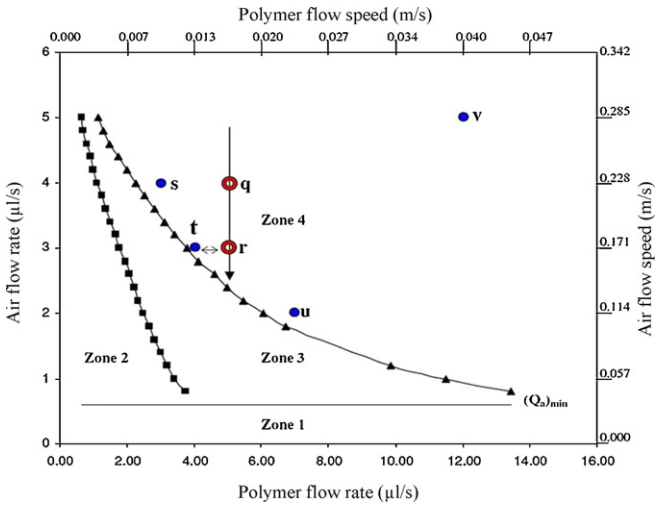

Fig. 1. Parametric plot of the relationship between the flow rate of air and the flow rate of 18 wt.% polymer solution. Zone 1: No microbubbling due to insufficient air. Zone 2: No microbubbling due to insufficient liquid. Zone 3: Intermittent microbubbling and Zone 4: Continuous microbubbling. The letters q, r, s, t, u and v represent the flow rate combinations at which CEHDA microbubbling was performed, and are defined in the text. The other two axes represent same data (air flow and polymer flow speed) with the unit of ms^{-1}.

2.3. Microbubbling apparatus

The details of the co-axial electrohydrodynamic microbubbling experimental set-up is found in Farook et al. (2008). In brief, the polymer solution was pumped through an outer capillary needle while air was passed through the inner capillary. The flow rates of air and polymer solution were regulated by high precision Harvard syringe pumps (PHD 4400) which were connected to two syringes with different capacities, 10 ml for air and 5 ml for polymer solution. A high voltage DC power supply was connected to both the capillaries relative to an earthed ring electrode placed 12 mm below the outer needle. The flow of the materials was monitored on a screen using a LEICA S6D JVC-colour video camera attached to a zoom lens and a DVD video recorder MP-600.

2.4. Process and product characterization

A parametric plot constructed between the flow rate of air and the flow rate of polymer solution provided the basis for this investigation (Fig. 1). Comparison of the size and size distribution of microspheres was made after microbubbling the polymer solution–air system at six different combinations of flow rates chosen from the parametric plot. These flow rate combinations are represented by letters q, r, s, t, u and v in Fig. 1. Products prepared at each flow rate combination were collected in glass vials of distilled water kept just below the ring electrode for the formation of microspheres. Samples of 0.05 ml of the suspension were taken from the glass vials using 1 ml syringes and transferred to glass slides and dried under ambient temperature and atmospheric pressure for 2 h and then in a desiccator for 2 days. Subsequently, these were used for scanning electron microscopy (JEOL JSM-6301F field emission scanning electron microscope).

Table 1
Properties of the 18 wt.% polymer solution.

Density (kg m^{-3})	Viscosity (mPa s)	Surface tension (mN m^{-1})	Electrical conductivity (Sm^{-1}/10^5)
845	2.5	23	9

3. Results and discussion

All experiments reported in this work were conducted using the 18 wt.% polymer solution (Table 1). In our previous study, four different concentrations (18 wt.%, 24 wt.%, 40 wt.% & 60 wt.%) were microbubbled and compared (Farook et al., 2008). The 18 wt.% solution was found to provide the largest applied voltage range over which there was no solidification of polymer at the needle tip during microbubbling, due to its moderate electrical conductivity and low surface tension (Farook et al., 2008). This enabled stable electrohydrodynamic microbubbling, with all three sequential modes of microbubble evolution, namely bubble dripping, coning and microbubbling, over a wide range of applied voltages (4.9–5.7 kV) (Farook et al., 2007a,b). The polymer solutions containing >18 wt.% polymer were difficult to microbubble due to their lower electrical conductivity and the rapid solidification of the polymer at the capillary exit. For instance, it was observed that at 40 wt.%, the polymer began to solidify at the tip of the outer needle in a range of applied voltage of 0–4.7 kV and this phenomenon was more noticeable at 60 wt.% solutions.

A parametric plot was constructed between the air flow rate and the polymer solution flow rate using 18 wt.% solution (Fig. 1). In Zone 1, due to the lack of sufficient gas phase, the polymer solution behaved as if it was subjected to conventional electrohydrodynamic atomization and therefore, no microbubbling occurred below this critical minimum air flow rate of 0.6 μL s^{-1}. Also, in Zone 2 due to the low flow rates of liquid, no microbubbling was observed. In Zone 3, the microbubbling was intermittent and unstable but continuous and stable microbubbling was achieved in Zone 4. The combinations of flow rates denoted by q and r were chosen for further investigation within the continuous microbubbling region (Zone 4) of the parametric plot.

The scanning electron micrographs of the microspheres prepared at the flow rate combinations represented by q and r are shown in Fig. 2a and c. The corresponding size distribution data obtained by measuring 300 microspheres from these micrographs are given in Fig. 2b and d and the respective flow rates, flow ratio (air/liquid), mean diameter, standard deviation and polydispersivity index (P.I.) are shown in Table 2. The mean size of the fabricated microspheres slightly reduced from 0.5 μm (at point q) down to 0.4 μm (at point r which is closer to the threshold of the continuous microbubbling zone). The polydispersivity index of the sample r was dramatically lower (50%) compared to the P.I. of the sample q. Thus, via a systematic manipulation of the flow rate of the air, more monodisperse microspheres were produced.

Points s, t and u were chosen on both sides of the vertical line and closer to the threshold boundary of the continuous microbubbling zone in order to compare the results achieved at point r with the size and size distribution of microspheres obtained at other possible combinations of flow rates that can result in smaller particles. The point v is chosen to represent a combination of higher flow rates. The results obtained are summarised in Table 3.

The scanning electron micrographs of the microspheres prepared at flow rate combinations with respect to points s, t, and u are given in Fig. 3a, c and e. The corresponding size distribution data measuring ~300 microspheres from these micrographs are given in Fig. 3b, d and f. The scanning electron micrograph with respect to point v is given in Fig. 3g. It was observed that microspheres prepared at flow rate combinations near the continuous bubbling threshold (s, t, u), were more polydisperse with higher standard deviation. In the case of t, it is very close to the line demonstrating the continuous to intermittent microbubbling transition zone and this seems to significantly increase the polydispersivity even though the flow ratio is very similar to the value at q and r. At s and u the flow ratio used is higher and lower respectively, compared with point r and this has increased the polydispersivity. The mean size, standard deviation and polydispersivity of the samples prepared at v (Fig. 1) were relatively high and seems to be dominated by the use of a high polymer flow rate. These results indicate point r lies in the optimum region for obtaining microspheres with low standard deviation and polydispersivity.

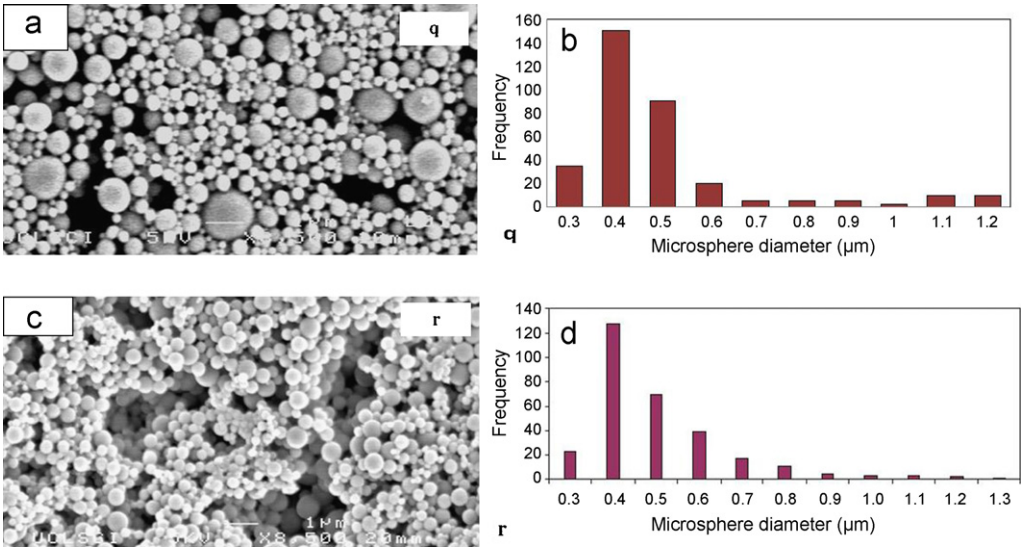

Fig. 2. Scanning electron micrographs of microspheres prepared under ambient temperature and pressure and flow rate combinations at q with air:polymer flow rate of 4 μL s^{-1}:5 μL s^{-1} (a) and at r with air:polymer flow rate of 3 μL s^{-1}:5 μL s^{-1} (c). Size distribution data obtained by measuring ~300 microspheres from respective scanning electron micrographs (b & d).

Table 2
Processing conditions for co-axial electrohydrodynamic microbubbling of 18 wt.% polymer solution at ambient conditions and size data of microspheres obtained.

Position on parametric plot	Flow rate of air ($\mu L s^{-1}$)	Flow rate of polymer ($\mu L s^{-1}$)	Flow ratio (λ)	Mean diameter (μm)	Standard deviation (μm)	P.I. (%)
q	4	5	0.8	0.50	0.08	16
r	3	5	0.6	0.40	0.03	8

Table 3
Microsphere sizes obtained by co-axial electrohydrodynamic microbubbling of 18 wt.% polymer solution at ambient conditions where flow rate combinations were selected near the continuous microbubbling threshold (s, t, u) and v represents a combination of higher flow rates.

Position on parametric plot	Flow rate of air ($\mu L s^{-1}$)	Flow rate of polymer ($\mu L s^{-1}$)	Flow ratio (λ)	Mean diameter (μm)	Standard deviation (μm)	P.I. (%)
s	4	3	1.33	0.9	0.20	22
t	3	4	0.75	0.52	0.34	39
u	2	7	0.29	0.50	0.08	16
v	5	12	0.42	1.2	0.62	52

The results shown in Tables 2 and 3 suggest two important points. First, a detailed investigation of a parametric plot can facilitate identification of flow rate combinations that will result in much smaller microspheres with a very low polydispersivity index fulfilling the main objective of preparing microspheres of submicrometre size with a narrow size distribution. Second, it is not the flow ratio which always determines the size of the spheres but also the absolute magnitude of the flow rates. For instance, although the flow ratio at point v is slightly smaller and comparable to the flow ratio at r (~0.6), the mean sphere size (1.2 μm) generated was much larger and accompanied by a very high polydispersivity index (52%) due to the high magnitudes of flow rates that lead to larger jet diameters at the time of microbubbling (Farook et al., 2007b). At a fixed voltage of 5.7 kV, within the continuous microbubbling region (Zone 4) and

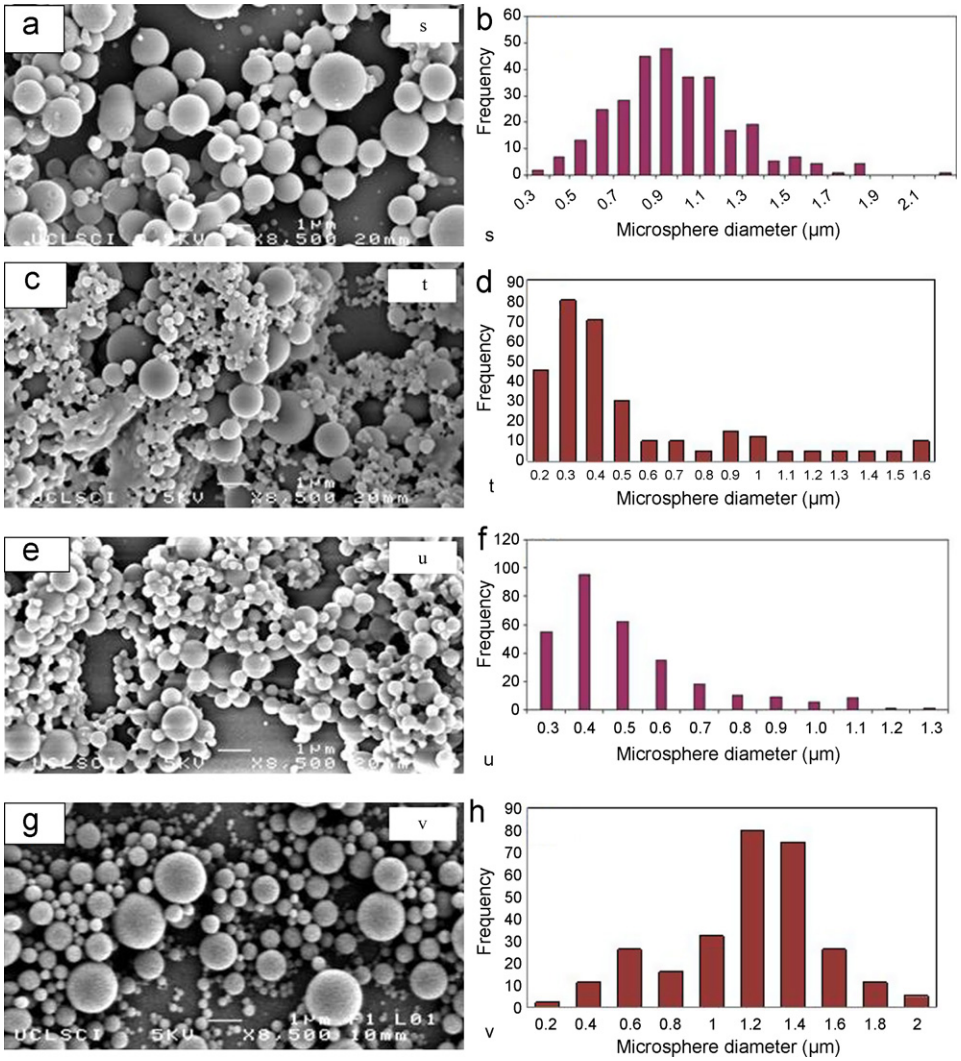

Fig. 3. Scanning electron micrographs of microspheres prepared at s with air:polymer flow rate of 4 μL s−1:3 μL s−1 (a), t with air:polymer flow rate of 3 $\mu L s^{-1}$:4 $\mu L s^{-1}$ (c), u with air:polymer flow rate of 2 $\mu L s^{-1}$:7 $\mu L s^{-1}$ (e) & v with air:polymer flow rate of 5 $\mu L s^{-1}$:12 $\mu L s^{-1}$ (g). Size distribution data obtained by measuring 300 microspheres from respective scanning electron micrographs (b, d, f & h).

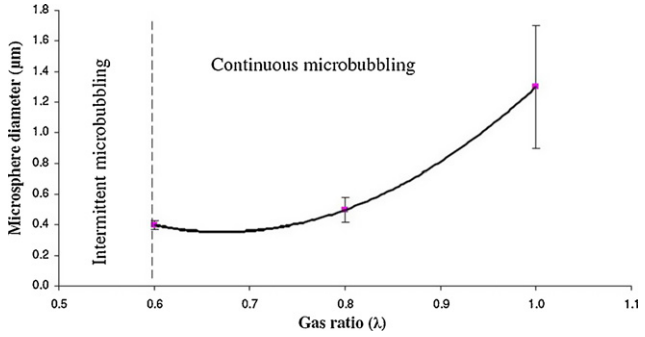

Fig. 4. Graph of the microsphere diameter (db) versus the flow ratio (λ) within the continuous microbubbling zone (gas ratio between 0.6 and 1) of the parametric plot.

on the vertical line passing through point q, the mean microsphere diameter d_b, for the polymer solution–air system, scales with the flow ratio λ according to the equation (Fig. 4):

$$d_b = 8.75(\lambda - 0.67)^2 + 0.35 \quad (1)$$

The ability to mass produce polymeric microspheres with a mean diameter of 400 nm with a narrow size distribution is of clinical significance (Amiji, 2006). The authors' previous work on microbubbling shows that the rate of production is at least 10^9 capsules per minute. As such, the results obtained in this investigation could be considered as an important milestone in preparing polymeric therapeutic agent (drug, gene or cell) delivery vehicles using CEHDA microbubbling. However, since the diameter of the microspheres limits the area of application of the microspheres, the demand for much smaller spheres is also equally high. Since CEHDA microbubbling is dependent on many variables such as process parameters, material parameters, needle geometry, ground electrode configuration and collection distance, it would be always possible to carry out further investigations by making changes in all these parameters to further tailor the characteristics of the products. Current and on-going parallel investigations in our laboratory have also shown how the internal structure of the carriers prepared can be controlled from particulates (Enayati et al., 2010, 2009) to hollow spheres (Chang et al., 2010a) and filled with different active pharmaceutical ingredients (API) such as estradiol, insulin and celecoxib. At a more generic level, we have simulated the release of a standard dye used in drug release studies (Pancholi et al., 2009; Chang et al., 2010b) and aim to match the molecular weight of this dye with APIs having similar, higher or lower molecular weights.

4. Conclusions

The results of this study show that co-axial electrohydrodynamic atomization microbubbling can be used to prepare spheres in the submicrometre range with a narrow size distribution. A parametric plot was constructed between the air flow rate and the polymer solution flow rate using a 18 wt.% polymer solution. The optimum region for obtaining microspheres with low standard deviation was identified. The lowest mean diameter of the spheres prepared in this work was 0.4 μm with a polydispersivity index of 8%. The size and size distribution could be further reduced by varying other process parameters such as the polymer concentration, needle size and collection distance and the aim of further work is to achieve drug-filled nanocapsules <100 nm in diameter with a polydispersivity index of <1%.

Acknowledgements

Marjan Enayati thanks UCL for part-funding her PhD research. We would also like to thank the Engineering and Physical Sciences Research Council (UK) and the Royal Academy of Engineering for sponsoring our drug delivery research work.

References

Amiji, M.M., 2006. Active Targeting Strategies in Cancer with a Focus on Potential Nanotechnology Applications 'Nanotechnology for cancer therapy', New York, NY 10016, pp. 19–37.
Arbós, P., Arangoa, M.A., Campanero, M.A., Irache, J.M., 2002. Quantification of the bioadhesive properties of protein-coated PVM/MA nanoparticles. Int. J. Pharm. 242, 129–136.
Bibby, D.C., Davies, N.M., Tucker, I.G., 1999a. Investigations into the structure and composition of b-cyclodextrin:poly(-acrylic acid) microspheres. Int. J. Pharm. 180, 161–168.
Bibby, D.C., Davies, N.M., Tucker, I.G., 1999b. Poly(acrylic acid)microspheres containing b-cyclodextrin: loading and in vitro release of two dyes. Int. J. Pharm. 187, 243–250.
Blanco, M.D., Gomez, C., Olmo, R., Muniz, E., Teijion, J.M., 2000. Chitosan microspheres in PLG films as devices for cytarabine release. Int. J. Pharm. 202, 29–39.
Brannon-Peppas, L., 1997. Polymers in controlled drug delivery. Med. Plast. Biomater. 4, 34–44.
Chang, M.W., Stride, E., Edirisinghe, M., 2010a. Controlling the thickness of hollow polymeric microspheres prepared by electrohydrodynamic atomization. J. R. Soc. Interface 7, S377–S378.
Chang, M.W., Stride, E., Edirisinghe, M., 2010b. Stimulus-responsive liquids for encapsulation storage and controlled release of drugs from nano-shell capsules. J. R. Soc. Interface, 0428, doi:10.1098/rsif. 2010.
Desai, M.P., Labhasetwar, V., Amidon, G.L., Levy, R.J., 1996. Gastrointestinal uptake of biodegradable microparticles: effect of particle size. Pharm. Res. 13, 1838–1845.
Desai, M.P., Labhasetwar, V., Walter, E., Levy, R.J., Amidon, G.L., 1997. The mechanism of uptake of biodegradable mi-endocroparticles in caco-2 cells is size dependent. Pharm. Res. 14, 1568–1573.
Dunne, M., Corrigan, O.I., Ramtoola, Z., 2000. Influence of particle size and dissolution conditions on the degradation properties of polylactide-coglycolide particles. Biomaterials 21, 1659–1668.
Enayati, M., Ahmad, Z., Stride, E., Edirisinghe, M., 2010. Size mapping of electric field-assisted production of polycaprolactom particles. J. R. Soc. Interface 7, S393–S404.
Enayati, M., Ahmad, Z., Stride, E., Edirisinghe, M., 2009. Preparation of polymeric carriers for drug delivery with different shape and size using an electric jet. Curr. Pharm. Biotechnol. 10, 600–608.
Farook, U., Zhang, H.B., Edirisinghe, M.J., Stride, E., Saffari, N., 2007a. Preparation of microbubble suspensions by co-axial electrohydrodynamic atomization. Med. Eng. Phys. 29, 749–754.
Farook, U., Stride, E., Edirisinghe, M.J., Moaleji, R., 2007b. Microbubbling by co-axial electrohydrodynamic atomization. Med. Biol. Eng. Comput. 45, 781–789.
Farook, U., Edirisinghe, M.J., Stride, E., Colombo, P., 2008. Novel co-axial electrohydrodynamic in-situ preparation of liquid-filled polymer-shell microspheres for biomedical applications. J. Microencapsul. 25, 241–247.
He, Y., 2008. Application of flow-focusing to the break-up of an emulsion jet for the production of matrix-structured microparticles. Chem. Eng. Sci. 63, 2500–2507.
Hettiarachchi, K., Lee, A.P., 2010. Polymer-lipid microbubbles for biosensing and the formation of porous structures. J. Colloid Interface Sci. 344, 521–527.
Illum, L., Davis, S.S., Wilson, C.G., Thomas, N.W., Frier, M., Hardy, J.G., 1982. Blood clearance and organ deposition of intravenously administered colloidal particles—the effects of particle-size, nature and shape. Int. J. Pharm. 12, 135–146.
Jain, R.A., 2000. The manufacturing techniques of various drug loaded biodegradable poly(lactide-co-glycolide) devices. Biomaterials 21, 2475–2490.
Jalil, R., Nixon, J.R., 1990. Biodegradable poly(lactic acid) and poly(lactide-co-glycolide) microcapsules: problems associated with preparative techniques and release properties. J. Microencapsul. 7, 297–325.
Jaworek, A., 2007. Micro- and nanoparticle production by electrospraying. Powder Technol. 176, 18–35.
Khutoryanskiy, V.V., 2007. Hydrogen-bonded interpolymer complexes as materials for pharmaceutical applications. Int. J. Pharm. 334, 15–26.
Lamprecht, A., Schafer, U., Lehr, C.M., 2001. Size-dependent bioadhesion of micro- and nanoparticulate carriers to the inflamed colonic mucosa. Pharm. Res. 18, 788–793.
Langer, R., 1990. New methods of drug delivery. Science 249, 1527–1533.
Lee, M.H., Lee, D., 2010. Elastic instability of polymer-shelled bubbles formed from air-in-oil-in-water compound bubbles. Soft Matter 6, 4326–4330.
May, R.C., Machesky, L.M., 2001. Phagocytosis and the actin cytoskeleton. J. Cell Sci. 114, 1061–1077.
Moghimi, S.M., Hunter, A.C., 2001. Long-circulating and target specific nanoparticles: theory to practice. J. C. Murray, Pharm. Rev. 53, 283–318.
Mitragotri, S., Lahann, J., 2009. Physical approaches to biomaterial design. Nat. Mater. 8, 15–23.
Pancholi, K., Stride, E., Edirisinghe, M., 2009. *In vitro* method to characterise diffusion from dye from polymeric particles: a model for drug release. Langmuir 25, 10007–10013.
Panyam, J., Dali, M.A., Sahoo, S.K., Ma, W.X., Chakravarthi, S.S., Amidon, G.L., Levy, R.J., Labhasetwar, V., 2003. Polymer degradation and in vitro release of a model protein from poly(D, L-lactide-co-glycolide) nano- and microparticles. J. Control. Release 92, 173–187.

Pareta, R., Edirisinghe, M.J., 2006. A novel method for the preparation of biodegradable microspheres for protein drug delivery. J. R. Soc. Interface 3, 573–582.
Park, T.G., Lee, H.Y., Nam, Y.S., 1998. A new preparation method for protein loaded poly(D,L-lactic-co-glycolic acid) microspheres and protein release mechanism study. J. Control. Release 55, 181–191.
Patil, V.R.S., Campbell, C.J., Yun, Y.H., Slack, S.M., Goetz, D.J., 2001. Particle diameter influences adhesion under flow. Biophys. J. 80, 1733–1743.
Pillai, O., Panchagnula, R., 2001. Polymers in drug delivery. Curr. Opin. Chem. Biol. 5, 447–451.
Rejman, J., Oberle, V., Zuhorn, I.S., Hoekstra, D., 2004. Size-dependent internalization of particles via the pathways of clathrin- and caveolaemediated endocytosis. Biochem. J. 377, 159–169.
Sahoo, S.K., Panyam, J., Prabha, S., Labhasetwar, V., 2002. Residual polyvinyl alcohol associated with poly (D,L-lactide-co-gly-colide) nanoparticles affects their physical properties and cellular uptake. J. Control. Release 82, 105–114.
Stolnik, S., Illum, L., Davis, S.S., 1995. Long circulating microparticulate drug carriers. Adv. Drug Deliv. Rev. 16, 195–214.
Stride, E., Edirisinghe, M., 2008. Novel microbubble preparation technologies. Soft Matter 4, 2350–2359.
Tabata, Y., Ikada, Y., 1990. Phagocytosis of polymer microspheres by macrophages. Adv. Polym. Sci. 94, 107–141.
Uhrich, K.E., Cannizzaro, S.M., Langer, R.S., Shakesheff, K.M., 1999. Polymeric systems for controlled drug release. Chem. Rev. 99, 3181–3198.
Wang, D., Robinson, D.R., Kown, G.S., Samuel, J., 1999. Encapsulation of plasmid DNA in biodegradable poly(D,L-lactic-co-strucglycolic acid) microspheres as a novel approach for immuno-gene delivery. J. Control. Release 57, 9–18.
Xie, J., Marijnissen, J.C.M., Wang, C.H., 2006. Microparticles developed by electrohydrodynamic atomization for the local delivery of anticancer drug to treat C6 glioma in vitro. Biomaterials 27, 3321–3332.
Xu, Y., Hanna, M.A., 2008. Morphological and structural properties of two-phase coaxial jet electrosprayed BSA-PLA capsules. J Microencapsul. 25, 469–477.
Zauner, W., Farrow, N.A., Haines, A.M., 2001. In vitro uptake of polystyrene microspheres: effect of particle size, cell line and cell density. J. Control. Release 71, 39–51.